

Technical note

# Synchrotron X-ray diffraction study on a single nanowire of PX-phase lead titanate

Tomoaki Yamada<sup>a,\*</sup>, Jin Wang<sup>b</sup>, Osami Sakata<sup>c</sup>, Cosmin S. Sandu<sup>b</sup>, Zhanbing He<sup>b</sup>, Takafumi Kamo<sup>a</sup>, Shintaro Yasui<sup>a</sup>, Nava Setter<sup>b</sup>, Hiroshi Funakubo<sup>a</sup>

<sup>a</sup> Department of Innovative and Engineered Materials, Tokyo Institute of Technology, 4259-J2-43, Nagatsuta-cho, Midori-ku, Yokohama 226-8502, Japan

<sup>b</sup> Ceramics Laboratory, Swiss Federal Institute of Technology, EPFL, CH-1015 Lausanne, Switzerland

<sup>c</sup> Japan Synchrotron Radiation Research Institute/SPring-8, Kouto, Sayo-cho, Hyogo 679-5198, Japan

Received 10 March 2010; received in revised form 20 June 2010; accepted 6 July 2010

Available online 3 August 2010

## Abstract

Synchrotron X-ray diffraction (XRD) measurements of Pb–Ti–O fine acicular crystals (nanowires) of the so-called PX-phase have been performed. The  $\theta$ – $2\theta$  patterns of the nanowires dispersed on substrates with two different geometries indicated that the PX-phase Pb–Ti–O nanowire has [1 1 0] along its short axis and [0 0 1] along its longitudinal axis. Using a focused micro-X-ray beam, we first demonstrated the XRD analysis of a single nanowire of PX-phase Pb–Ti–O. Bragg reflections from the same single nanowire with scattering vectors at two different angles suggested its tetragonal unit cell having the rather large *a*-axis lattice constant.

© 2010 Elsevier Ltd. All rights reserved.

**Keywords:** Pb–Ti–O; PZT; Fibers; X-ray methods; Piezoelectric properties

## 1. Introduction

Perovskite lead titanate and lead zirconate titanate are well known ferroelectric and piezoelectric materials, and therefore used for the wide variety of applications.<sup>1</sup> Recent researches of these materials are more focused on the form of thin films due to the requirement of minimization of the existing devices and the additional functionalities into on-wafer devices. However, it has become clear that the ferroelectricity and piezoelectricity are significantly influenced by the clamping of films owing to substrates.<sup>1–4</sup> The fine acicular or filiform crystals (i.e. nanowires) having less than submicron meter widths can be therefore of interest as ideal materials for those purposes since nanowires are completely free from the clamping effect.<sup>4,5</sup> In addition, they may even bring us the more pronounced properties than bulk materials due to their unique one-dimensional structures.<sup>6</sup>

Among the different ways to synthesis nanowires, the hydrothermal method offers a remarkably low temperature process, especially in comparison with the vapor-phase growth methods such as sputtering and chemical vapor deposition. However, by the hydrothermal method, it has been known to be difficult to produce lead titanate (Pb–Ti–O) nanowires with perovskite phase; instead, a so-called PX phase can be grown.<sup>7,8</sup> This PX-phase Pb–Ti–O uniquely appears in the form of nanowires, and the powder X-ray diffraction (XRD) indicates that it has a tetragonal body-centered unit cell.<sup>7,8</sup> While these few findings have been reported, many questions arise: What orientation does the PX-phase Pb–Ti–O nanowire have? Does XRD of a bunch of nanowires with different sizes prove the tetragonal unit cell of PX-phase Pb–Ti–O? Is there neither ferroelectricity nor piezoelectricity in PX-phase Pb–Ti–O? There are several analytical methods on the nanometer scale for exploring such questions, for instance, transmission electron microscope (TEM), piezo force microscopy and micro Raman spectroscopy; each has advantages but none of them is versatile. In this report, we first demonstrate the XRD analysis of a ‘single’ nanowire of PX-phase Pb–Ti–O using a micro-X-ray beam of synchrotron radiation. XRD with the beam size similar to the nanowire can provide a strong possibility to clarify structural properties of

\* Corresponding author.

E-mail addresses: [yamada.t.al@m.titech.ac.jp](mailto:yamada.t.al@m.titech.ac.jp) (T. Yamada), [jin.wang@epfl.ch](mailto:jin.wang@epfl.ch) (J. Wang), [o-sakata@spring8.or.jp](mailto:o-sakata@spring8.or.jp) (O. Sakata).

those individual nanowires, including the orientation, precise lattice constants and symmetry. The approach used can also be extended to reveal their piezoelectric properties in the future, by monitoring the lattice distortion under an applied electric field.

## 2. Experimental

PX-phase Pb–Ti–O nanowires were fabricated by the hydrothermal method. The 40 mL feedstock consisting of  $0.10 \text{ mol l}^{-1}$  of  $\text{TiO}(\text{OH})_2$  that was hydrolyzed from  $\text{Ti}(\text{OC}_4\text{H}_9)_4$ ,  $0.11 \text{ mol l}^{-1}$  of  $\text{Pb}(\text{NO}_3)_2$ ,  $0.5 \text{ mol l}^{-1}$  of KOH and  $0.4 \text{ g l}^{-1}$  of polyvinyl alcohol (PVA) solution was prepared, and was then charged into a 50 ml stainless-steel Teflon-lined autoclave for a hydrothermal treatment at  $200^\circ\text{C}$  for 5 h. The products were filtered and washed by deionized water and absolute ethanol, and dried at  $45^\circ\text{C}$  in air.

For XRD measurements, we used synchrotron X-rays with 12.4 keV photon energy (wavelength is approximately 0.1 nm) in SPring-8 BL13XU. The SPring-8 is located at Hyogo in Japan and the largest third-generation synchrotron radiation facility in the world. An 8-GeV storage ring of the SPring-8 allows us to brilliant and pulsed X-rays; therefore, the diffraction intensities from a small amount of nanowires can be detected. The nanowires were dispersed on fused silica substrates and polyimide tape substrates as below described in detail. To focus the X-rays onto a single nanowire, the X-ray beam size was scaled down to a few micrometers using the two-dimensional focusing refractive lens system made from an SU-8 resist on a Si wafer substrate (Forschungszentrum Karlsruhe).<sup>9,10</sup>

## 3. Results and discussion

Fig. 1 shows the scanning electron microscope (SEM) image of the nanowires fabricated. The nanowires with a square pole-shape (namely, with a rectangular cross-section)<sup>11</sup> having sizes in the range of  $100 \text{ nm}–1 \mu\text{m}$  width and  $6 \mu\text{m}–40 \mu\text{m}$  length were observed by SEM and TEM (not shown here). A powder XRD pattern of the nanowires (not shown here) basically agreed with the data reported by Cheng et al.<sup>8</sup>

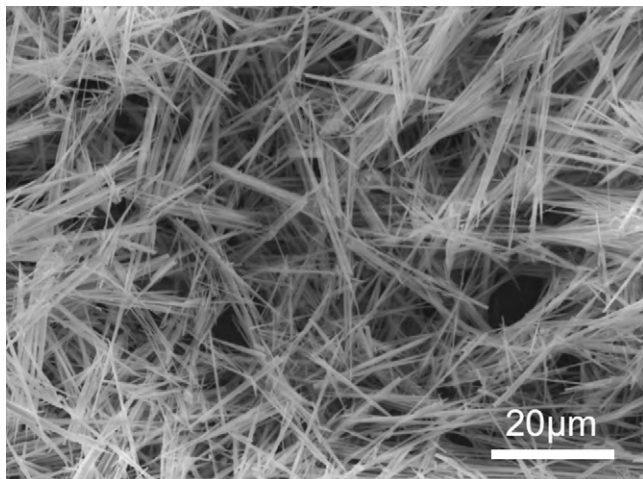


Fig. 1. SEM image of PX-phase Pb–Ti–O nanowires.

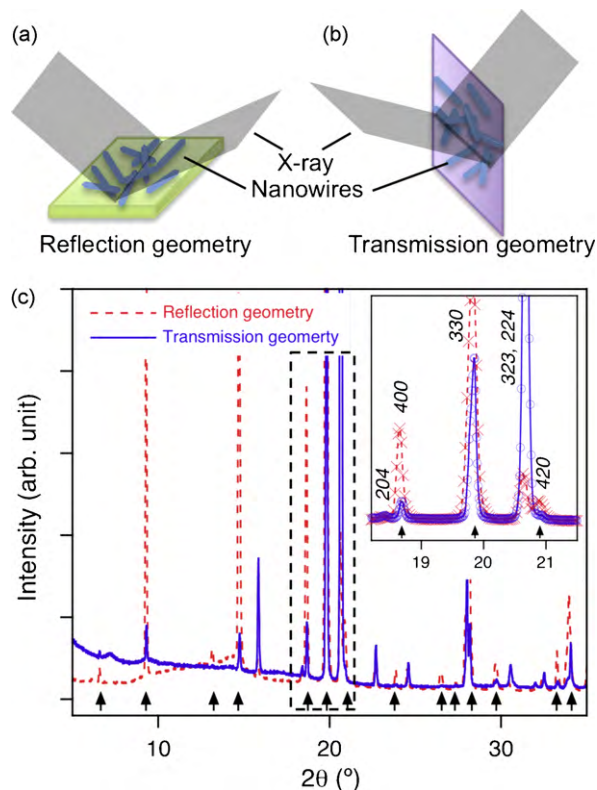


Fig. 2. Schematic illustration for XRD  $\theta$ – $2\theta$  scans with two different geometries: reflection geometry (a) and transmission geometry (b). (c) The  $\theta$ – $2\theta$  patterns obtained from PX-phase Pb–Ti–O nanowires with the geometries shown in (a) and (b). The arrows show the angular positions for  $h k 0$  peaks.

Due to the geometrical feature of nanowires, the nanowires are laid on the flat substrate when they are dispersed. This allows us to estimate the crystal orientation of these nanowires from XRD with two kinds of geometries using a X-ray beam with a size  $\sim \text{mm}^2$  covering multiple nanowires:  $\theta$ – $2\theta$  scans with a reflection geometry (for which a scattering vector is perpendicular to the substrate surface, see Fig. 2a) and a transmission geometry (for which a scattering vector is parallel to the substrate surface, see Fig. 2b). The former will preferentially give the diffraction intensities from the lattice planes parallel to the longitudinal direction of nanowire, and the latter will rather equally give the diffraction intensities from all the planes. For the measurements with the reflection geometry, the nanowires were dispersed in isopropanol to form a suspension, and then dried on the fused silica substrates. We confirmed that the nanowires were lying on the substrate by microscope. For the transmission geometry, the nanowires on the fused silica substrates were transferred to the polyimide tape substrates to be able to efficiently transmit X-rays through the substrate. Fig. 2c shows the  $\theta$ – $2\theta$  XRD patterns of PX phase Pb–Ti–O nanowires with the two different geometries. Both XRD patterns have peaks at the same  $2\theta$  angles; nevertheless, the intensity ratio of peaks was significantly different for these geometries. As especially clearly found in the inset of Fig. 2c, the intensities of  $h k 0$  peaks such as 400, 330 and 420 indicated by arrows are larger for the reflection geometry, while the  $h k l$  ( $l \neq 0$ ) peak intensities are

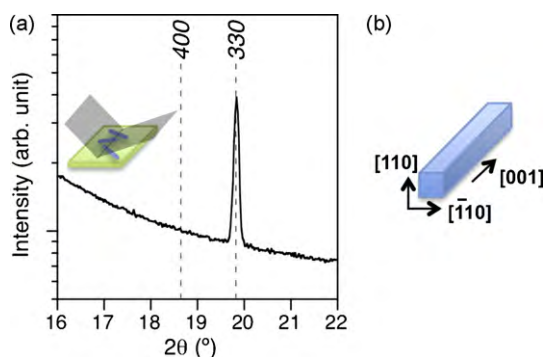


Fig. 3. XRD  $\theta$ - $2\theta$  pattern with the reflection geometry for (400) and (330) planes of the nanowires thinly dispersed on the substrate (a). Suggested crystal orientation of PX-phase Pb-Ti-O nanowire (b).

larger for the transmission geometry. This result indicates that  $[hk0]$  is perpendicular to the longitudinal axis of the nanowires, and therefore,  $[001]$  will be along the longitudinal direction. In order to clarify the orientation along the short axis, the  $\theta$ - $2\theta$  scan for (400) and (330) planes with the reflection geometry has been performed for the nanowires more thinly dispersed on the substrate so that nanowires did not overlap each other as schematically illustrated in Fig. 3a. In this case, the short edges of the most of nanowires with square pole-shape are naturally placed parallel and perpendicular to the substrate surface (see Fig. 3b). In Fig. 3a, the very strong 330 peak was found while the 400 peak was negligibly recorded. The results evidently suggest that the PX-phase Pb-Ti-O nanowire has  $[110]$  along its short axis and  $[001]$  along longitudinal axis, as illustrated in Fig. 3b. Our recent TEM observation of the similar nanowires of PX-phase Pb-Zr-Ti-O<sup>11</sup> and a very recent report on TEM observation of PX-phase Pb-Ti-O nanowires by Zhu et al.<sup>12</sup> also support the present study using the fast and nondestructive way by synchrotron XRD.

For the further detailed characterizations, the structural analysis of a single nanowire is necessary. Using a tiny but highly bright X-ray beam of synchrotron radiation, we found that the detection of a single PX-phase Pb-Ti-O nanowire was possible. Fig. 4 shows the intensity profile of the incident micro-X-ray beam obtained from knife edge scans, for which the gold plate having sharp edges cut across the X-ray beam vertically or hori-

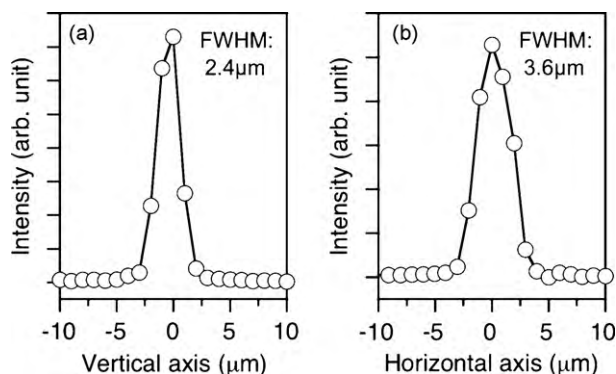


Fig. 4. Intensity profile of the micro-X-ray beam along vertical direction (a) and horizontal direction (b) obtained from the knife edge scans.

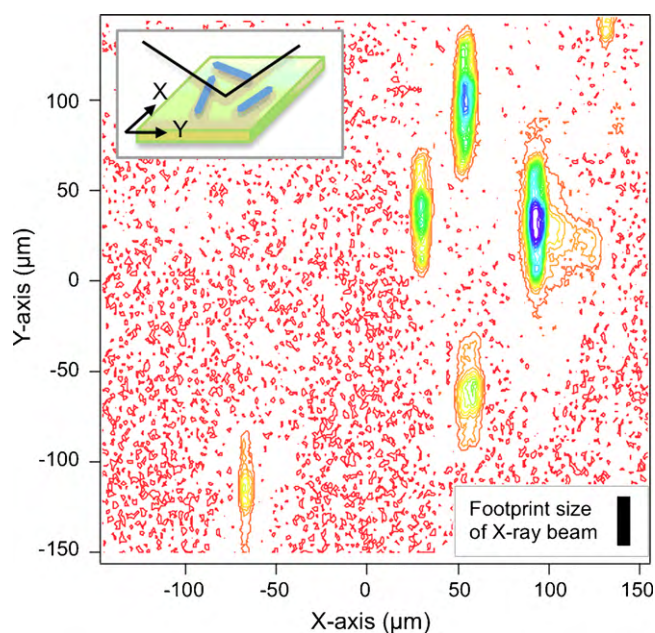


Fig. 5. Two-dimensional mapping ( $300\mu\text{m} \times 300\mu\text{m}$  area) of the (330) diffraction intensity for PX-phase Pb-Ti-O nanowires dispersed on the substrate, using a micro-X-ray beam. The footprint of X-ray beam (in the full width) is also illustrated.

zontally. The FWHM beam width was  $2.4\mu\text{m}$  and  $3.6\mu\text{m}$  along its vertical and horizontal directions, and the full width is about twice larger along each direction. Fig. 5 shows the surface mapping of the diffraction intensity for the (330) Bragg reflection of PX-phase Pb-Ti-O nanowires using the micro-X-ray beam. As clearly seen in the figure, the diffraction spots from each single nanowire have been observed. Because of the larger footprint of the X-ray beam on the substrate than the original beam size due to the incident angle of  $9.9^\circ$  for the (330) Bragg reflection (see the illustration in the figure), these diffraction spots are elongated along the incident beam direction. Therefore, the shape of the spot does not exactly reflect that of each nanowire especially when smaller than the footprint. Nevertheless, this 2-dimensional mapping enables us to focus the X-ray beam only on a single nanowire.

Fig. 6 shows the  $\theta$ - $2\theta$  scans for  $(hh0)$  and  $(h00)$  lattice planes of the same single nanowire for which scattering vectors are perpendicular to the surface (Fig. 6a) and are tilted by  $45^\circ$  from the surface (Fig. 6b), respectively. The former revealed only  $hh0$  peaks and the latter revealed only  $h00$  peaks, showing the single crystal nature of the nanowire. The lattice spacing for (100) and (110) was estimated to be  $12.343\text{Å}$  and  $8.726\text{Å}$ , respectively. On the basis of the fact that the angle between the (100) and (110) scattering vectors was  $45^\circ$ , the (010) lattice spacing can be calculated to be  $12.34\text{Å}$ , which accords with the (100) lattice spacing within the accuracy of the measurement. We also confirmed that the (100)/(010) lattice spacing is basically in agreement with the value reported by Cheng et al.<sup>8</sup> The results obtained from a single nanowire indicate that the PX-phase Pb-Ti-O nanowire has a tetragonal unit cell ( $a=b \neq c$ ,  $\alpha=\beta=90^\circ$ ) with rather large  $a$ -axis lattice constant.

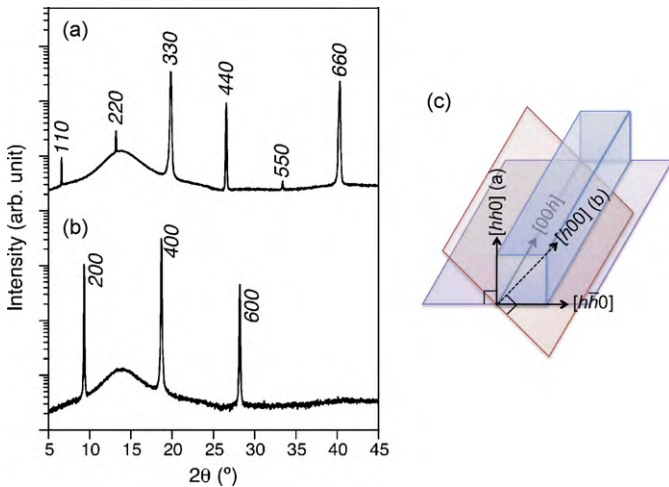


Fig. 6. XRD  $\theta$ - $2\theta$  patterns for  $(hh0)$  planes (a) and  $(h00)$  planes (b) from the same single nanowire. Scattering vectors are perpendicular to the surface (a) and are tilted by  $45^\circ$  from the surface (b), as schematically illustrated in (c).

#### 4. Conclusions

We have demonstrated synchrotron XRD measurements of PX-phase Pb-Ti-O nanowires. By comparing the diffraction patterns of the nanowires dispersed on the substrates with reflection and transmission geometries, the crystal orientation of PX-phase Pb-Ti-O nanowires was found to be  $[1\ 1\ 0]$  along its short axis and  $[0\ 0\ 1]$  along its longitudinal axis. The micro-X-ray beam of synchrotron radiation enabled us to distinguish each nanowire dispersed on the substrate; therefore, the XRD analysis of a single nanowire have been achieved for the first time. The  $\theta$ - $2\theta$  scans with two different scattering vectors of the same single nanowire suggested its tetragonal unit cell having rather large  $a$ -axis lattice constant. The obtained results show that the micro-XRD is a very strong tool for the clarification of the structural properties of nanowire. Although there is no clear answer judging if the PX-phase Pb-Ti-O nanowire has piezoelectricity at this time, the used approach can also be extended for the study on the electromechanical property by monitoring the lattice distortion under an electric field to seek its piezo-activity.

#### Acknowledgements

The work of TY was supported by Global COE program at Tokyo Institute of Technology. The work of JW and NS is supported by the Swiss National Science Foundation. The synchrotron radiation experiments were performed at the BL13XU in the SPring-8 with the approval of the Japan Synchrotron Radiation Research Institute (JASRI) (Proposal Nos. 2008A1590 and 2009A1027).

#### References

1. Setter N, Damjanovic D, Eng L, Fox G, Gevorgian S, Hong S, et al. Ferroelectric thin films: review of materials, properties, and applications. *J Appl Phys* 2006;**100**, 051606-1-46.
2. Nagarajan V, Stanishevsky A, Chen L, Zhao T, Liu B-T, Melngailis J, et al. Realizing intrinsic piezoresponse in epitaxial submicron lead zirconate titanate capacitors on Si. *Appl Phys Lett* 2002;**81**:4215-7.
3. Buhlmann S, Dwir B, Baborowski J, Muralt P. Size effect in mesoscopic epitaxial ferroelectric structures: increase of piezoelectric response with decreasing feature size. *Appl Phys Lett* 2002;**80**:3195-7.
4. Li J-H, Chen L, Nagarajan V, Ramesh R, Roytburd AL. Finite element modeling of piezoresponse in nanostructured ferroelectric films. *Appl Phys Lett* 2004;**84**:2626-8.
5. Wang J, Stampfer C, Roman C, Ma WH, Setter N, Hierold C. Piezoresponse force microscopy on doubly clamped  $\text{KNbO}_3$  nanowires. *Appl Phys Lett* 2008;**93**:223101-1-3.
6. Hong J, Fang D. Systematic study of the ferroelectric properties of  $\text{Pb}(\text{Zr}_{0.5}\text{Ti}_{0.5})\text{O}_3$  nanowires. *J Appl Phys* 2008;**104**:064118-1-5.
7. Uedaira, S, Suzuki, M, Yamanoi, H, Tamura, H, Method for manufacturing fine lead titanate powders. European Patent 186199, 2 July, 1986.
8. Cheng H, Ma J, Zhao Z, Qiang D, Li Y, Yao X. Hydrothermal synthesis of acicular lead titanate fine powders. *J Am Ceram Soc* 1992;**75**:1123-228.
9. Sakata O, Yasui S, Yamada T, Yabashi M, Kimura S, Funakubo S. In situ lattice-strain analysis of a ferroelectric thin film under an applied pulse electric field. *In AIP Conference Proceedings* 2010;**1234**:151-4.
10. Last A. *LIGA and its applications*, vol. 7. New York: Wiley, John & Sons; 2009. pp. 233-242.
11. Wang J, Sandu CS, Setter N. Large-scale fabrication of titanium-rich perovskite PZT submicro/nano wires and their electromechanical properties. *IEEE Trans Ultrason Ferroelectr Freq Control* 2009;**56**:1813-9.
12. Zhu X, Xing Z, Zhang Z, Zhu J, Song Y, Zhou S, et al. Microwave-hydrothermal synthesis and structural characterization of PX-phase single-crystalline  $\text{PbTiO}_3$  nanowires by electron microscopy. *Mater Lett* 2010;**64**:479-82.